JOURNAL OF GEOPHYSICAL RESEARCH, VOL. 104, NO. A6, PAGES 12,339-12,349, JUNE 1, 1999

Formation and evolution of subauroral ion drifts in the course of a substorm

J. De Keyser

Belgian Institute for Space Aeronomy, Brussels

Abstract. We propose a physical mechanism that explains how "polarization jets" (PJ) or "subauroral ion drifts" (SAID) are formed in the course of a substorm and how they evolve. A PJ/SAID is considered to be the ionospheric signature of an inward moving injected plasma front. The flow shear that exists across this interface when it arrives in the vicinity of the plasmapause is responsible for the generation of intense electric fields in the premidnight sector, where PJ/SAID are observed. Quantitative simulation of this mechanism accounts for PJ/SAID width and peak drift velocity. The mechanism explains why PJ/SAID are observed poleward of or in the vicinity of the plasmapause. The inward traveling time of the injected plasma agrees with the delay between substorm onset and the apparition of PJ/SAID; the evolution of the ionospheric signature is consistent with observations as well.

1. Introduction

Substorms often lead to the formation of narrow layers of intense westward drift in the subauroral ionosphere. These structures are known as "polarization jets" (PJ) or "subauroral ion drift layers" (SAID) [*Galperin et al.*, 1973; *Burch et al.*, 1976; *Smiddy et al.*, 1977; *Maynard*, 1978; *Spiro et al.*, 1979; *Rich et al.*, 1980; *Anderson et al.*, 1991; *Yeh et al.*, 1991; *Karlsson et al.*, 1998]. They have a narrow latitudinal extent and are characterized by a westward drift speed in excess of 1 km s^{-1}, by a temperature peak due to collisions between the drifting particles and neutral atoms, and by an ionospheric density trough. PJ/SAID are located equatorward of the nightside auroral zone and poleward of or in the vicinity of the plasmapause (PP). PJ/SAID are usually observed more than half an hour after the onset of a magnetospheric substorm and last less than 3 hours. Although the ionospheric signature of PJ/SAID is reasonably well understood [*Galperin et al.*, 1986; *Filippov et al.*, 1989; *Rodger et al.*, 1992; *Anderson et al.*, 1993], the electromotive force driving the phenomenon has not yet been identified satisfactorily.

The theory of magnetospheric convection based on tracing the drift paths of individual charged particles in the magnetospheric electric field predicts an energy-dependent evolution of the "injection boundary" [*McIlwain*, 1974] because of the dispersion of ions and electrons of different temperatures. This leads to the formation of a space-charge layer (Alfvén layer), which carries shielding currents because of the nonzero ionospheric conductivity [*Block*, 1966; *Jaggi and Wolf*, 1973; *Gurevich et al.*, 1976; *Southwood and Wolf*, 1978]. Attempts have been made to relate the ionospheric phenomena observed in PJ/SAID to properties of this Alfvén layer [*Spiro et al.*, 1981; *Anderson et al.*, 1993; *Ober et al.*, 1997]. It appears, however, that the dispersion of particles injected at a given point in the near-Earth tail is significant. *Karlson* [1971] obtains an Alfvén layer thickness of the order of 1 R_E. Moreover, the injection process deposits these particles in a certain volume rather than at a single point. The space-charge layer will therefore be relatively thick, making it hard to adequately explain the narrow latitudinal extent of PJ/SAID layers.

In the present paper we focus on the microphysics of the injected particle front. We demonstrate that finite gyroradius effects at this interface [*Lemaire et al.*, 1998; *De Keyser et al.*, 1998] are responsible for creating fine-scale structure, allowing us to view the narrow PJ/SAID as the ionospheric signature of such an earthward moving magnetospheric interface between cold plasma trough and hot injected particles. The azimuthal shear flow between the injected plasma and the partially corotating plasma trough in the vicinity of the plasmapause and the thermoelectric effects at the interface are identified as the key ingredients for the formation of the intense electric fields inside PJ/SAID.

This paper is organized as follows: We first discuss the nature of a magnetospheric interface between cold plasma trough and hot injected plasma. We then explain the origin of the electric field inside such an interface and its ionospheric signature. We present simulations confirming the quantitative agreement of this mechanism with observations. We end with a discussion of the implications of the proposed mechanism.

2. PJ/SAID as Ionospheric Signature of a Magnetospheric Interface

PJ/SAID are layers of intense westward ion drift (> 1 km s^{-1}) and poleward electric field (> 50 mV m^{-1}), observed

Paper number 1999JA900109.
0148-0227/99/1999JA900109$09.00

in the F region and higher. Collisional heating inside such layers can cause the formation of a stable auroral red arc [*Foster et al.*, 1994]. The production of NO^+ [*Schunk et al.*, 1975] and its fast recombination with electrons depletes the charge carriers, thereby reducing the ionospheric conductivity [*Banks and Yasuhara*, 1978; *Anderson et al.*, 1993]. The physicochemical timescale of these processes is of the order of minutes [*Anderson et al.*, 1991].

PJ/SAID are associated with magnetospheric substorms [*Spiro et al.*, 1979; *Anderson et al.*, 1993; *Karlsson et al.*, 1998]. While increased drifts are observed during the expansion phase, the spike signature typical of PJ/SAID appears only in the early recovery phase, more than half an hour after substorm onset [*Anderson et al.*, 1993]. PJ/SAID generally last less than 3 hours [*Maynard et al.*, 1980; *Anderson et al.*, 1991], although an occasional lifetime of 6 hours has been reported [*Yeh et al.*, 1991]. PJ/SAID occur between 1600 and 0300 hours local time (LT), most often in the dusk and premidnight sectors [*Spiro et al.*, 1979; *Karlsson et al.*, 1998]. Their azimuthal extent ranges from about 1 to 6 hours LT. The poleward electric field inside PJ/SAID implies the existence of a potential drop across the layer. PJ/SAID are threaded to the magnetosphere by highly conducting magnetic field lines; in the absence of a possible ionospheric driver, it is therefore natural to look for a driving electromotive force in the magnetosphere. Simultaneous observations of conjugate PJ/SAID in the Northern and Southern Hemispheres [*Anderson et al.*, 1991] also suggest a common magnetospheric source.

2.1. Electric Circuit

Figure 1 shows, for the Northern Hemisphere, how the dipolar ionospheric magnetic field $\mathbf{B}_{\text{iono}}$ points down (where $B_{\text{iono}} = B_{\text{eq}}(1 + 3\sin^2\lambda)^{1/2}/(1 + h/R_E)$, where λ is the invariant latitude (ILAT), h is the altitude, and $B_{\text{eq}} = 3.11 \times 10^{-5}$ T is the equatorial field strength at the Earth's surface), while the ion drift $\mathbf{V}_{\text{iono}}$ is directed westward. Given the low ionospheric collision rate, the drift is mainly the result of a poleward electric field $\mathbf{E}_{\text{iono}}$:

$$\mathbf{V}_{\text{iono}} = \mathbf{E}_{\text{iono}} \times \mathbf{B}_{\text{iono}}/B_{\text{iono}}^2.$$

Similarly, a poleward electric field exists in PJ/SAID in the Southern Hemisphere. Because $\mathbf{B}_{\text{iono}}$ does not vary appreciably across the PJ/SAID, the $\mathbf{V}_{\text{iono}}$ and $\mathbf{E}_{\text{iono}}$ profiles are similar. The ionospheric electric potential difference $\Delta\Phi$ ranges from a few to tens of kilovolts [*Smiddy et al.*, 1977; *Spiro et al.*, 1979; *Karlsson et al.*, 1998]. In magnetic latitude aligned PJ/SAID whose azimuthal extent is much larger than their width (the usual case), we can ignore border effects; the azimuthal current is zero. Downward field-aligned currents flow on the equatorward side of the PJ/SAID, Pedersen currents flow through the ionosphere (a resistive load), and field-aligned currents flow upward on the poleward side. The height-integrated current along the latitude-aligned drift band is

$$J \approx \frac{\Delta\Phi}{2\Delta\lambda}\frac{\Sigma}{R_E + h},$$

where $\Delta\lambda$ is the latitudinal width of the PJ/SAID and Σ is the height-integrated ionospheric Pedersen conductivity. For typical values $\Sigma = 0.3$ S, $\Delta\Phi = 20$ kV, $\Delta\lambda = 0.5°$, and $h = 400$ km, the current is $J = 0.05$ A m^{-1} along the westward drift band [*Smiddy et al.*, 1977; *Rich et al.*, 1980; *Anderson et al.*, 1993]. A PJ/SAID can therefore be regarded as the ionospheric footprint of a field-aligned current sheet

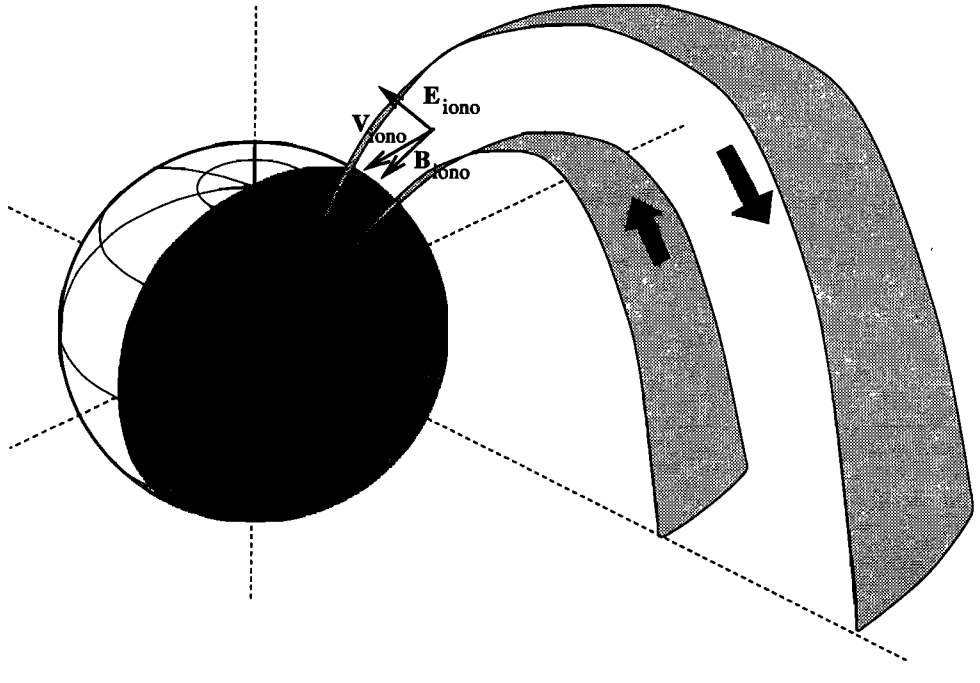

Figure 1. Schematic view of the current sheet connecting the nightside ionosphere where a PJ/SAID is observed to the magnetosphere. The ionospheric magnetic field $\mathbf{B}_{\text{iono}}$ points down, the ionospheric drift $\mathbf{V}_{\text{iono}}$ is westward, and the electric field $\mathbf{E}_{\text{iono}}$ is directed poleward. The arrows indicate the direction of the field-aligned and ionospheric currents.

connecting the PJ/SAID to its magnetospheric source. The power deposited in the ionosphere is $J\,\Delta\Phi \approx 1000$ W m^{-1} along the PJ/SAID band. Accounting for the reduced ionospheric conductivity inside PJ/SAID, the field-aligned currents and the power drawn from the source can be somewhat smaller [*Banks and Yasuhara*, 1978; *Anderson et al.*, 1993]; the lifetime of the source is correspondingly longer. Whenever one of both ionospheric footprints is sunlit (where the ionospheric conductivity is not negligible), the dissipated power remains considerable. This may help to explain the semi-annual variation in observed PJ/SAID electric field strength [*Karlsson et al.*, 1998].

2.2. Observation of Injected Plasma

A magnetic substorm can be triggered by a change of the interplanetary magnetic field direction. The development of an X-type neutral line in the near-Earth tail (at $20 - 30\ R_E$) leads to the acceleration of plasma both sunward and tailward and is responsible for the "bursty bulk flow" in the magnetotail [*Angelopoulos et al.*, 1992]; earthward flows exceeding 100 km s^{-1} have been reported [*Frank et al.*, 1994; *Ho et al.*, 1994].

Storm-time observations of flux dropouts in geostationary orbit ($L = 5.7$) prior to or during observations of PJ/SAID events in the ionosphere in the same local time sector [*Anderson et al.*, 1993] suggest the presence of hot injected plasma sheet material in the inner magnetosphere. Similar flux dropouts are reported by *Shiokawa et al.* [1997]. Precipitation of energetic particles all the way down from the auroral region to the PJ/SAID latitude [*Anderson et al.*, 1993] confirms the presence of hot plasma on the tailward side of the interface.

Maynard et al. [1980] report the observation by ISEE 1 of PJ/SAID-like electric fields at a magnetospheric interface just outside the plasmapause, at about 2300 LT, near the $L = 4$ drift shell. *De Keyser et al.* [1998] have shown that such electric fields can indeed be generated at a premidnight interface between hot injected plasma and the cold plasma trough.

2.3. Lifetime of the Electrostatic Field

The hot and cold ions and electrons at the magnetospheric interface have different gyroradii. The resulting charge separation provokes a polarization electric field inside the layer. The field-aligned currents closing through the ionosphere act so as to neutralize this charge separation. The polarized interface can be regarded as a capacitor that is discharged through the ionospheric resistance. *Willis'* [1970] study of a similar resistance-capacitance (RC) circuit for the magnetopause is applicable to PJ/SAID as well. He found the discharge time to be

$$\tau = \frac{\epsilon\epsilon_0 A}{d\,\Sigma} \ln\left(1 + \frac{d}{(R_E + h)\cos\Lambda}\right),$$

with a dielectric constant $\epsilon \approx [1 + (\omega_e/\Omega_e)^2]^{1/2} d/\lambda_D$. For a PJ/SAID at $\Lambda = 60°$ invariant latitude (at $L = 4$, where $B \approx 490$ nT), the surface of the magnetospheric interface with an azimuthal extent $\Delta\varphi$ is $A \approx (\Delta\varphi/2\pi) \times 2 \times 10^{14}$ m^2. The Debye length is $\lambda_D \approx 2$ m for a 1 eV plasma with a number density of 10 cm^{-3}. The electron plasma frequency is $\omega_e \approx 2 \times 10^5$ rad s^{-1}, and the electron gyrofrequency $\Omega_e \approx 10^5$ rad s^{-1}. With a distance $d \approx 10$ km between the polarization charges (length scale in between the hot and cold proton gyroradii) and a height-integrated conductivity $\Sigma \approx 0.1$–1 S, we find $\tau \approx 10$–100 s. The discharge time cannot be much smaller, as the propagation of electromagnetic signals at Alfvén speed along the magnetic field lines connecting the source to the load already takes several seconds.

An alternative way to compute the discharge time is the following [*De Keyser et al.*, 1998]. The gradients responsible for the electrostatic field at the interface will disappear when a significant fraction (say, 50 %) of the particles within the interface layer is evacuated; evacuation is slowest for the cold particles. With a plasma trough density of $N = 10$ cm^{-3} at the outer edge of the plasmapause, at $L = 4$, a flux tube with unit cross section in the equatorial plane contains 10^{15} particles (adopting an r^{-4} plasmaspheric density profile). Assuming thermal particle transport away from the equator and toward the ionosphere and adopting the maximum precipitation loss (a full loss cone), the flux tube evacuation rate is $R_{\rm loss} = N\,V_{\rm th} \approx 6 \times 10^{11}$ m^{-2} s^{-1} for 0.75 eV electrons and 2×10^{11} m^{-2} s^{-1} for 1.5 eV protons. A field-aligned potential drop can further enhance this rate, so that $R_{\rm loss} \approx 10^{12}$ m^{-2} s^{-1}. Precipitating protons and electrons both contribute to a field-aligned current density $2eR_{\rm loss} \approx 3 \times 10^{-7}$ A m^{-2}. The observed ionospheric field-aligned current densities of the order of 1 μA m^{-2} [*Smiddy et al.*, 1977] do indeed imply a current density of 10^{-7}–10^{-8} A m^{-2} in the equatorial magnetosphere. From the flux tube particle content and the loss rate we derive an evacuation time $\tau = 10^2$–10^3 s, comparable to the result found earlier.

The discharge timescale τ is too short to account for the observed lifetime of PJ/SAID. Because of the inward motion of the magnetospheric interface, however, the polarization charges are continuously replenished from the plasma reservoirs on either side. In a frame comoving with the interface, the plasma on either side is flowing toward the current sheet and is ejected along the field lines. The influx of cold particles into the flux tube at $L = 4$ is determined by the projected surface of the flux tube in the inward direction ($A \approx 10^7$ m^2 per unit length along the azimuthal direction), by the plasma trough number density ($N = 10$ cm^{-3}), and by the thickness of the layer ($D \approx 1000$ km, projected from the observed ionospheric PJ/SAID width). As the particle loss equals the number of cold particles swept up by the inward moving front, the velocity of the interface must be

$$V_{\rm in} = R_{\rm loss} D/AN,$$

which is ≈ 10 km s^{-1}. Such a modest inward velocity is sufficient to maintain the current circuit. The structure of the magnetospheric interface is not essentially modified by the field-aligned currents as long as the injected plasma reservoir is not exhausted and its inward motion is not completely stopped. The ionospheric conductivity therefore is not nec-

essarily the most important element determining the lifetime of the PJ/SAID structure. The long-lived dynamic equilibrium in which the effects of ionospheric discharge and constant replenishment cancel can then be modeled in a first approximation by a tangential discontinuity (TD) equilibrium in which discharge and replenishment are ignored.

2.4. Inward Motion of Injected Plasma

Anderson et al. [1993] state that minor ionospheric signatures are observed during substorm expansion, at progressively lower latitudes, until finally a PJ/SAID appears. At the same time, the precipitation region is observed to extend to progressively lower latitudes. We interpret these observations as manifestations of the inward motion of the injected plasma. The injected plasma front pushes aside the cold plasma trough plasma on its way inward. When the azimuthal extent of the injected plasma front is large, sideways motion of the cold plasma is only important at the flanks of the plasma front; the cold plasma is pushed away mainly along the magnetic field lines and will precipitate. Since the particle content of plasma trough flux tubes ahead of the plasma front increases on its way inward, while the plasma trough temperature and the loss rate decrease, the interface must slow down. At the plasmapause, where the density increases up to 1000 cm^{-3} [*Carpenter*, 1963], the inward speed drops to only 0.1 km s^{-1}; that is, the interface is not expected to propagate far across the plasmapause. Observations of energetic particle penetration during substorms up to and slightly beyond the plasmapause into the plasmasphere corroborate this scenario [*Ejiri et al.*, 1980]. This argument implies that once the ionospheric signature has developed into a PJ/SAID, the equatorward motion of this signature has essentially stopped.

One can model the plasma front as an Alfvén wave, which propagates inward with a speed

$$V_{\text{in}} = \frac{B_n}{\sqrt{\mu_0 m^+ N}} \tag{1}$$

if one ignores temperature anisotropy. Below, we always evaluate this expression using the plasma trough density; strictly speaking, some average of the plasma trough and injected plasma densities should be used. A velocity $V_{\text{in}} =$ 10 km s^{-1} at $L = 4$ implies a normal magnetic field component of only $B_n = 1.4$ nT, that is, $B_n/B = 0.003$, justifying the TD model as a first approximation for describing the internal structure of such a current layer. A rotational discontinuity (RD) model with small B_n implies that particles from the plasma trough as well as injected plasma can cross the interface, but their drift in the normal direction is so slow (relative to the interface) that they remain confined to a rather narrow layer: This is very similar to a TD geometry with appropriately chosen "trapped" populations [*Roth et al.*, 1996].

We now use equation (1) with a constant $B_n = 1$ nT to trace the inward motion of the injected plasma from the plasma sheet to the plasmapause. The time it takes for the injected plasma to arrive at the plasmapause is given by

$$\Delta t = \frac{\sqrt{\mu_0 m^+}}{B_n} \int_{r=R_{\text{PS}}}^{R_{\text{PP}}} \sqrt{N} dr;$$

R_{PP} and R_{PS} denote the positions of the plasmapause and the beginning of the plasma sheet, respectively. We model the density profile by $N(r) = N_{\text{PP}} \exp[(r - R_{\text{PP}})/\delta]$, where N_{PP} is the plasmaspheric density and $\delta \approx 1\ R_E$ is the length scale of the density change; this choice mimics the observed density profile for moderate K_p. We then find

$$\Delta t = \frac{2\delta}{B_n} \sqrt{\mu_0 m^+ N_{\text{PP}}} [1 - \exp(-\frac{R_{\text{PS}} - R_{\text{PP}}}{2\delta})].$$

With $N_{\text{PP}} = 1000\ \text{cm}^{-3}$, $R_{\text{PP}} = 4\ R_E$, and $R_{\text{PS}} = 10\ R_E$, the traveling time is $\Delta t \approx 1430$ s. This result is not very sensitive to R_{PP} and R_{PS} but strongly depends on B_n and δ. Associating the time of plasma injection with substorm onset, this traveling time is consistent with the observed half an hour delay between onset and PJ/SAID apparition [*Anderson et al.*, 1993].

2.5. Precipitation Boundary

Observations show that during substorm expansion the precipitation region extends down to lower latitudes, but the precipitation boundary remains always slightly poleward of the PJ/SAID band. This can be understood from the present model by the following reasoning. The PJ/SAID ionospheric electric field is an almost instantaneous signature of the magnetospheric electric field (Alfvén waves travel along the field lines in a matter of seconds). We now estimate the timescale of precipitation. Because of the conservation of the magnetic moment, the perpendicular velocity of the injected particles increases proportional to L^3. Conservation of the second adiabatic invariant implies a parallel velocity proportional to the field line length. The velocity distribution of the injected particles therefore becomes "pancake" shaped, with maximum phase space density near 90° pitch angle. Because of this flattening of the pitch angle distribution, the mean parallel velocity is an order of magnitude lower than the average thermal velocity, which is 19,000 and 1400 km s^{-1} for 1 keV electrons and 10 keV protons of plasma sheet origin. For $L = 4$ we find precipitation times of 20 and 300 s for these electrons and protons. For an inward velocity of the plasma front of 10 km s^{-1}, this implies that the precipitation signature lags behind the electric field signature over an equivalent magnetospheric distance of 200–3000 km, which is of the order of the transition thickness: the precipitation boundary is located poleward of the PJ/SAID but not far away.

3. Electric Field at the Interface

We have already shown that the magnetospheric interface can be modeled in a first approximation as a TD. In order not to complicate the discussion unnecessarily, we assume it to be locally planar with its normal in the radial direction. The structure of such a TD depends on the nature of the velocity distribution functions of the particles in the interface [*Whipple et al.*, 1984; *Roth et al.*, 1996]. An important de-

termining factor is the electric field inside the layer. There are two main contributions to this electric field: A polarization field due to finite gyroradius effects and a convection electric field arising from tangential flow on both sides of the interface.

3.1. Finite Gyroradius Effects

Finite gyroradius effects associated with the different energies of the ions and electrons involved lead to thermoelectric charge separation; this effect is particularly important because of the strong temperature gradient at the interface. Consider cold plasma trough plasma ($T_{\rm pt}^- = 0.75$ eV and $T_{\rm pt}^+ = 1.5$ eV [*Comfort*, 1996]) and hot injected plasma of plasma sheet origin ($T_{\rm in}^- = 1$ keV and $T_{\rm in}^+ = 10$ keV). The transition lengths $\mathcal{L}$, the length scales over which the population densities vanish across the current sheet, are of the order of the corresponding gyroradius or larger ($\mathcal{L} \geq \rho$) [*Roth et al.*, 1996]. We have taken the same values of $\mathcal{L}^+/\rho^+$ and $\mathcal{L}^-/\rho^+$ for the hot and cold protons and electrons, respectively. Note that $\mathcal{L}^+/\mathcal{L}^- = 0.1...10$ in order to avoid excessive electric fields that would provoke instabilities. We made the choice $\mathcal{L}^+/\rho^+ = 50$ and $\mathcal{L}^-/\rho^+ = 10$. The thickness of the layer is determined by the hot protons; it is of the order of $\mathcal{L}_{\rm in}^+ \approx 50\rho_{\rm in}^+ \approx 1500$ km, which maps down to about $\Delta\lambda = 1°$ ionospheric latitudinal width. The choice of $\mathcal{L}^+$ therefore matches the observed PJ/SAID thickness. The theoretical minimum thickness is obtained for $\mathcal{L}^+/\rho^+ = 1$, and then $D = 30$ km, and $\Delta\lambda = 0.02°$; the observed thickness is consistently larger.

Figure 2a sketches the electrostatic field in the transition when there is no flow shear, for the case $\mathcal{L}_{\rm pt}^- < \mathcal{L}_{\rm pt}^+ < \mathcal{L}_{\rm in}^- < \mathcal{L}_{\rm in}^+$ that corresponds to the chosen transition length values. The electric field peaks inside the layer. As the excess space charge δN is usually of the order of $10^{-6}N$, the peak thermoelectric field is $E_{x,\rm th-el} \approx \mathcal{L}_{\rm pt}^+ e\delta N/\epsilon_0 \approx 3$ mV m^{-1}.

3.2. Velocity Shear

The electric field in the injected plasma region must vanish in a comoving reference frame. This is accomplished by collective polarization effects inside the injected plasma region, generating surface charges in a thin shell at the injected plasma boundary. The hot particles are (partially) "shielded" from the external magnetospheric electric field; only particles in the surface layer experience this external field. Consequently, the hot plasma will not follow the drift trajectories traced by individual particles: Its deceleration and deflection upon approaching the plasmapause are retarded, and it can "hit" the plasmapause (see Figure 3). An azimuthal velocity shear ΔV therefore develops across the interface. Assuming that the injected plasma (moving sunward with velocity $V_{\rm in}$) decelerates in the immediate vicinity of a circular plasmapause (where the corotation velocity is $V_{\rm pt} = 2\pi R_{\rm PP}/T$, with $T = 1$ day, in the case of a rigidly corotating plasmasphere), this velocity shear is

$$\Delta V(\varphi) = V_{\rm in} \sin\varphi + V_{\rm pt}.$$

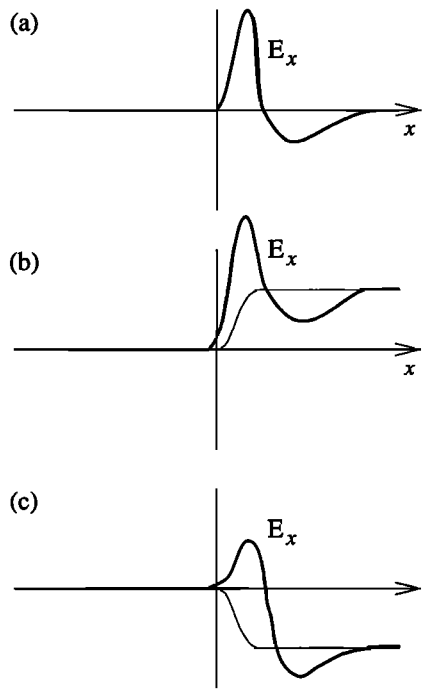

Figure 2. The electric field inside the magnetospheric interface layer: (a) thermoelectric field (no flow shear); (b) convection electric field for negative ΔV (thin line, premidnight configuration) and total electric field (thick line), where the electric field inside the layer is intensified; and (c) convection electric field for positive ΔV (thin line, postmidnight configuration) and total electric field profile (thick line). From *De Keyser et al.* [1998].

The injected plasma velocity and the corotation velocity are parallel at the dawnside; at the duskside, however, they are antiparallel, so that a large flow shear may develop there; the premidnight–postmidnight asymmetry is evident.

Figure 2b illustrates what happens when a shear flow corresponding to the premidnight configuration is present. In the frame of reference corotating with the cold plasma, the positive convection electric field $E_{x,\rm conv} = \Delta V\, B \approx 5$ mV m^{-1} (for $B = 490$ nT and $\Delta V = 10$ km s^{-1}) intensifies the electric field peak inside the layer to $E_x \approx 8$ mV m^{-1}. In the postmidnight local time sector the convection and thermoelectric fields tend to cancel (Figure 2c). This asymmetry in the intensity of the electric fields inside the layer, depending on the sense of the shear flow, also contributes to the premidnight–postmidnight asymmetry. Particularly intense fields are produced for the sense corresponding to the premidnight configuration and can even prohibit the existence of TD equilibrium [*De Keyser and Roth*, 1997]; as the inward motion of the injected plasma is decelerated at the plasmapause, while the plasma catches up with the azimuthal corotation, the velocity shear decreases, so that the TD equilibrium approximation always becomes justified from some point on.

In conclusion, the flow shear tends to be largest in the premidnight sector, and there it also has the sense most apt to produce a strong electric field peak. Both effects can explain the premidnight occurrence of PJ/SAID.

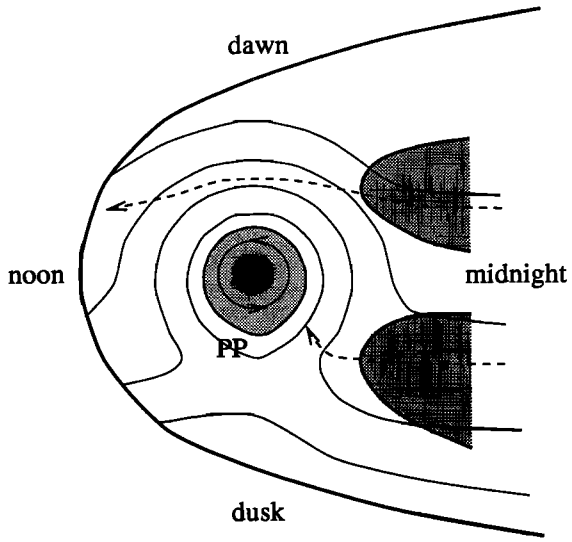

Figure 3. Motion of the injected plasma front through the magnetosphere. The thin lines sketch the global magnetospheric electric equipotentials (similar to *McIlwain*'s [1986] E5D model for moderate K_p). Because of collective effects, the injected plasma does not follow individual charged particle trajectories (that is, the equipotential surfaces) but deceleration and deflection upon approach of the plasmapause (PP) are delayed. In the premidnight sector, the injected plasma front may hit the plasmapause.

3.3. Ionospheric Signature

The potential difference $\Delta\Phi$ across the magnetospheric interface maps down into the ionosphere if the field-aligned potential drop is negligible; that is, if the magnetospheric resistivity and/or the field-aligned currents are small. As the dipolar magnetic field lines converge toward the ionosphere, the electric field across the interface at $L = 4$ is amplified by a factor $2L\sqrt{L-1} \approx 14$ when projected to the ionosphere. For a magnetospheric peak of 8 mV m^{-1} the ionospheric field becomes $E_{\text{iono}} = 110$ mV m^{-1}. The corresponding drift velocity $V_{\text{iono}} = -E_{\text{iono}}/B_{\text{iono}}$ ($B_{\text{iono}} \approx 6 \times 10^{-5}$ T) is -2 km s^{-1}. Such ionospheric electric fields and westward drifts are actually observed in PJ/SAID. Note that the mapping factor for an interface farther tailward is larger (for example, the factor is about 42 for $L = 8$). Weak electric fields at a distant interface can become significant when projected into the ionosphere and can give rise to secondary signatures [*Spiro et al.*, 1979].

4. Quantitative Model

In this section we quantitatively compute the electric field at the magnetospheric interface and the corresponding ionospheric drift. This requires a microscopic description of the interface.

4.1. A Quasi-Stationary Current Sheet Model

As discussed in section 2.3, the magnetospheric interface can be regarded as a TD. We take the evolution of the interface to be quasi-stationary; that is, subsequent snapshots correspond to equilibrium configurations. This is justified since the lifetime of the PJ/SAID phenomenon is of the order of hours, larger than the discharge time and the ionospheric physicochemical timescale. Quasi-stationarity implies pressure balance across the interface. We use a kinetic one-dimensional equilibrium TD model to compute the electric structure of the interface. The magnetic field is everywhere parallel to the sheet, and there is no plasma flow across it; the electric field points along the TD normal. We will use a right-handed reference frame comoving with the plasma trough, with x directed away from Earth and z to the north. The TD model is a simplified version of the more general model discussed by *Roth et al.* [1996] and is similar to magnetopause TD models [*Kuznetsova et al.*, 1994; *De Keyser and Roth*, 1997]. The velocity distribution functions in this model belong to a class of truncated Maxwellian distribution, parameterized by a transition length $\mathcal{L}$. The Vlasov-Maxwell equations are solved numerically using a variable-step integrator, as the problem involves widely different length scales.

4.2. Properties of Plasma Trough and Injected Plasma

Figure 4 shows the profiles of equatorial magnetospheric magnetic field, plasma trough density, and plasma trough

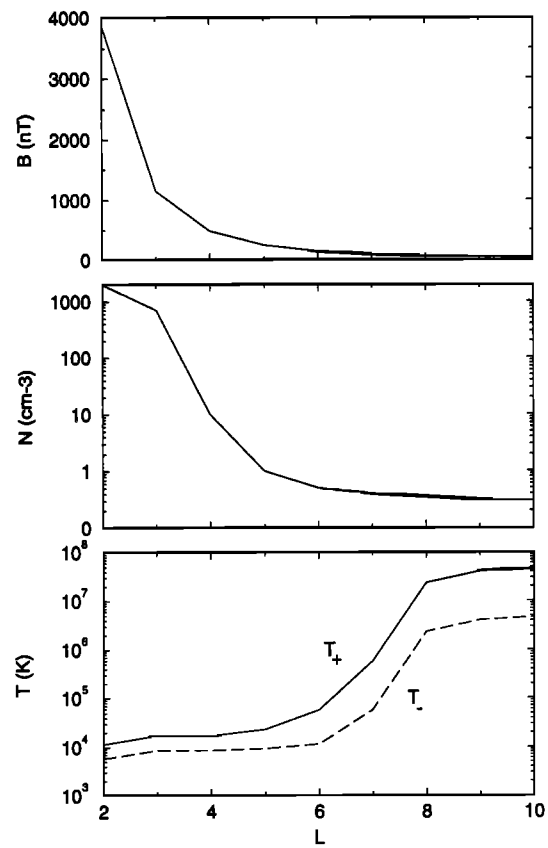

Figure 4. Typical midnight profiles of the magnetic field, the density, and the proton and electron temperatures (see also Table 1). The density gradient near $L = 4$ corresponds to the plasmapause.

proton and electron temperatures that we adopt in the model calculations (see also Table 1). These profiles correspond to moderate K_p values, with the plasmapause at $L = 3$–4. We consider the plasma trough and the injected plasma to consist each of one proton and one electron population. The plasma trough probably is better modeled by including a minor fraction of warm plasma [*Comfort*, 1996], but this would not alter the structure of the transition much. The properties of the injected plasma are less well known. We have adopted constant density and temperature values; this may not completely be justified because of adiabatic heating and a possible compression or expansion of the injected plasma on its way inward. Numerical experiments have confirmed, however, that the obtained electric fields and ion drifts are not very sensitive to these choices, as long as the injected plasma is outnumbered by the plasma trough plasma and is much hotter. In order to focus on the role of the electric field at the interface, we limit ourselves to the case where the magnetic field remains unidirectional; that is, it does not change orientation across the transition.

4.3. Injected Plasma Near the Plasmapause

Consider injected plasma reaching the plasmapause ($L = 4$) in the premidnight sector with a typical flow shear $\Delta V = -10$ km s^{-1} (this simulation is taken from *De Keyser et al.* [1998]). Figure 5a shows the number density profiles of the plasma trough protons and the less numerous injected protons. The hot particles affect the mean ion temperature over a distance of 4000 km earthward of the interface (Figure 5b). As the reference frame comoves with the plasma trough, the electric field (Figure 5c) is zero earthward of the interface and is positive in the injected plasma region. A strong peak is formed inside the layer, similar to the structure described in Figure 2b. The peak is about 1200 km wide. The ionospheric electric field is amplified owing to the convergence of the magnetic field lines, with a peak well over 100 mV m^{-1} (Figure 5d). We obtain a westward velocity peak exceeding 2 km s^{-1} concentrated in a region about 1° in latitude, located near 60° ILAT (Figure 5e). This is typical of PJ/SAID. It is remarkable that both PJ/SAID thickness and peak drift match the observations for a single value of $\mathcal{L}^+/\rho^+$.

Figure 6 considers the same injected plasma as before but now situated in the postmidnight sector. The shear flow has the opposite sense and is somewhat smaller ($\Delta V = +6$ km s^{-1}). The density and temperature gradients again reflect the disparity in transition lengths of the cold and hot populations (Figures 6a and 6b). The convection electric field is negative (Figure 6c). In agreement with the qualitative picture of Figure 2c, a pronounced electric field peak is absent. The ionospheric signature of this boundary layer (Figures 6d and 6e) therefore displays no ion drift velocity peak. This simulation confirms the ability of the proposed mechanism to explain the observed premidnight–postmidnight asymmetry.

4.4. Time Evolution of PJ/SAID Structure

We have traced the evolution of the ionospheric signature of the injected plasma front as it approaches the plasmapause by computing the drift profile for $L = 10$ down to $L = 4$ (parameters listed in Table 1; see also Figure 4). Successive drift profiles are shown as a ribbon plot in Figure 7. Invariant latitude ranges from 55° to 75° ILAT. The time elapsed since substorm onset (the time of injection) is obtained from equation (1). When the injected plasma is far away, the flow shear is zero, and there is no net electric potential drop across the interface (situation corresponding to Figure 2a). The magnetospheric electric field must then have a bipolar profile, which is reflected by the ionospheric drift velocity. The layer thickness is the combined result of the large magnetospheric width (small magnetic field implies large gyroradii) and the large mapping factor. As the injected plasma front moves inward, the latitude of the drift layer shifts equatorward. The flow shear increases, a potential drop develops across the transition, and the magnetospheric electric field as well as the ionospheric drift profiles become unipolar, leading to substantial ionospheric drifts. Strong and narrow drift peaks exceeding 1 km s^{-1} are formed only close to the plasmapause. This evolution fully agrees with observations [*Anderson et al.*, 1993].

As the plasmapause location depends on K_p, this scenario predicts that PJ/SAID will occur at lower latitudes when the plasmapause is closer to Earth, that is, when K_p is high.

Table 1. Magnetic Field and Plasma Data Used in the Simulations

L	B, nT	N_{pt}, cm^{-3}	T^+_{pt}, eV	T^-_{pt}, eV	N_{in}, cm^{-3}	T^+_{in}, keV	T^-_{in}, keV	ΔV, km s^{-1}
2	3887	2000	1.0	0.70	–	–	–	–
3	1152	700	1.2	0.70	–	–	–	–
4	486	10	1.5	0.75	1.00	10	1	-10.0
5	249	1	2	0.80	0.50	10	1	-6.5
6	144	0.50	5	1	0.30	10	1	-3.5
7	91	0.40	50	5	0.25	10	1	-2.0
8	61	0.35	2000	200	0.23	10	1	-1.0
9	43	0.31	3500	350	0.21	10	1	-0.5
10	31	0.30	4000	400	0.20	10	1	0

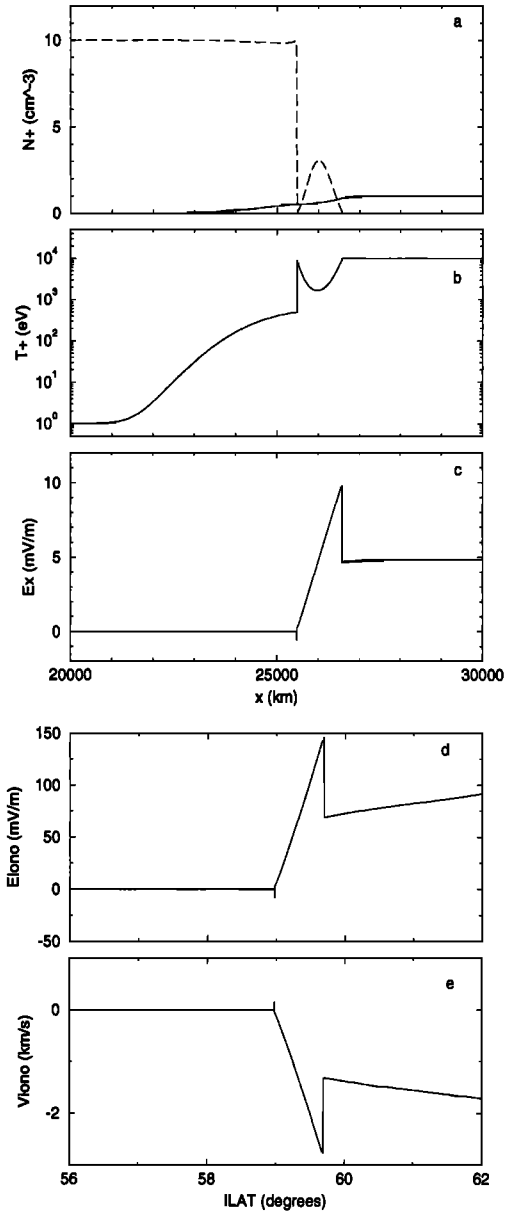

Figure 5. Structure of an injected plasma front in the premidnight sector at $L = 4$ computed with the tangential discontinuity model: (a) proton densities (dashed line shows cold magnetospheric plasma, and solid line shows injected plasma), (b) mean proton temperature, and (c) normal electric field as a function of geocentric distance, and (d) ionospheric electric field and (e) ionospheric drift as a function of invariant latitude (ILAT). From *De Keyser et al.* [1998].

Such a trend has indeed been observed [*Karlsson et al.*, 1998].

Yeh et al. [1991] discuss the westward drift bands in a double PJ/SAID event observed during a major substorm. The drift speed peak of the earthward PJ/SAID reached maximum intensity when the hot plasma first arrived at its innermost position, and it gradually decays afterward: The shear velocity is indeed expected to be largest upon arrival of the injected plasma close to the plasmapause but then decreases as energy is dissipated.

The evolution sketched above is also consistent with the observed broadening of the energetic electron precipitation region during a substorm; precipitation extends from the auroral zone down to the PJ/SAID latitude (see, for instance, Figure 1 of *Anderson et al.* [1993]), thus tracing the region pervaded by injected plasma.

5. Discussion and Conclusions

The purpose of this paper was to examine a scenario that explains the formation and evolution of subauroral ion drift

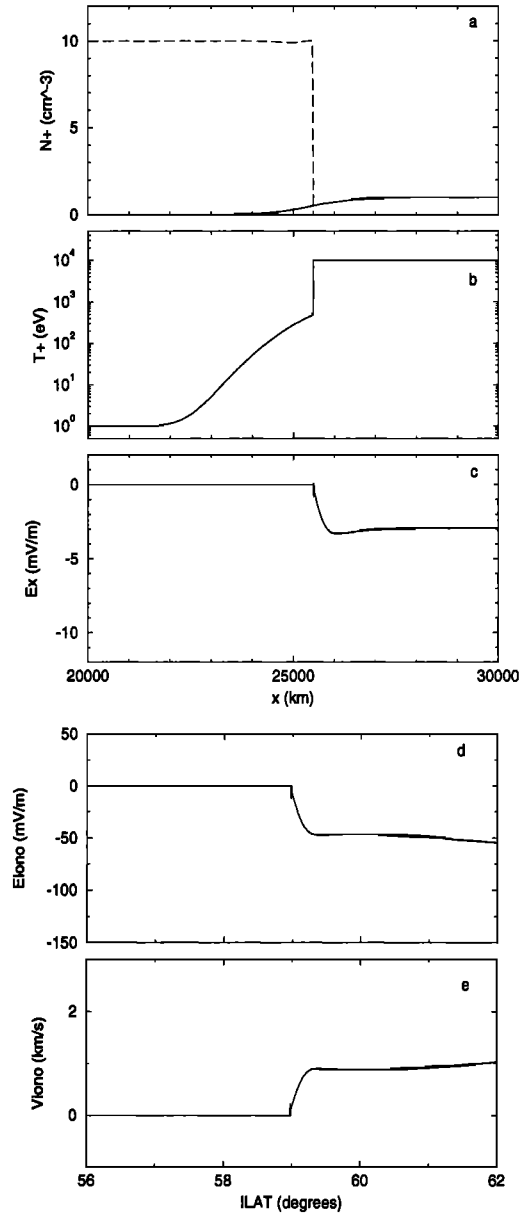

Figure 6. Structure of an injected plasma front in the postmidnight sector at $L = 4$ computed with the tangential discontinuity model: (a) proton densities (dashed line shows cold magnetospheric plasma, and solid line shows injected plasma), (b) mean proton temperature, and (c) normal electric field as a function of geocentric distance, and (d) ionospheric electric field and (e) ionospheric drift as a function of invariant latitude (ILAT).

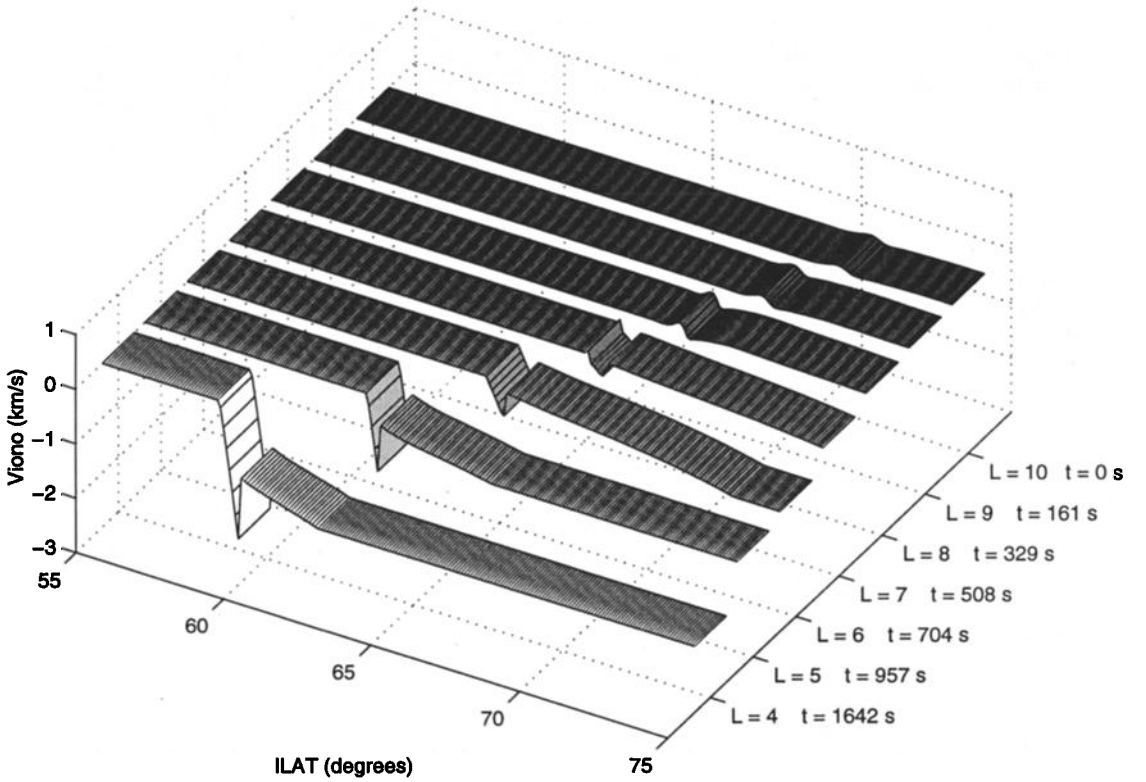

Figure 7. Evolution of the ionospheric drift as the injected plasma front moves in from $L = 10$ down to $L = 4$ (see Table 1 for simulation parameters). The ionospheric projection moves toward lower invariant latitudes (ILAT) as the injected plasma front moves inward while its width decreases and its strength increases. The time elapsed since onset is computed from equation (1).

layers in the storm-time magnetosphere: (1) Substorm onset leads to the injection of hot plasma sheet plasma. (2) In addition to global storm-time changes in the magnetospheric convection, thermoelectric effects produce a localized electric field at the injected plasma front, thus creating structure on the scale of the gyroradii of the particles involved. (3) An azimuthal flow shear develops across the interface as it moves inward, especially in the premidnight sector; the corresponding convection electric field enhances the electric field in the premidnight sector, but cancels electric field variations in the postmidnight sector. (4) As the inward motion proceeds, the ionospheric signature of the plasma front shifts equatorward. The drift profile develops a strong peak only when the front arrives in the vicinity of the plasmapause; this happens after an inward traveling time of about half an hour. (5) At the same time, the precipitation region reaches down to ever lower latitudes, with the precipitation boundary located slightly poleward of the ionospheric signature of the plasma front. (6) When the interface reaches the plasmapause, the inward motion slows down and intense electric fields are generated, leading to the apparition of a PJ/SAID. (7) The PJ/SAID structure progressively disappears while energy is dissipated in the ionosphere.

We have shown that the injected plasma front can be modeled in a good approximation as a tangential discontinuity. Qualitative and quantitative modeling demonstrates that the proposed scenario can account for many observed features of PJ/SAID: the width and peak intensities of the drift profile, the electric field, the field-aligned current densities, the gradual increase of the westward drifts as the phenomenon develops during substorm expansion, the observation of electric fields and flux dropouts in the magnetosphere in conjunction with PJ/SAID, the widening of the precipitation region, the delay between substorm onset and apparition of PJ/SAID, the latitude of PJ/SAID always poleward of or in the vicinity of the plasmapause, their premidnight occurrence, and the tendency of PJ/SAID to occur at lower latitudes with increasing K_p. While we have focused on the magnetospheric driver of the phenomenon, we have largely ignored the dynamics of the ionosphere by considering the unloaded electric circuit. *Deminov and Shubin* [1987, 1988], on the contrary, did not study the magnetospheric source but examined the dynamical response of the ionosphere to a plasma front that moves earthward instantaneously at the time of onset, with a prescribed potential drop across the front. Further progress could be made by studying the coupled system.

The merit of the present paper lies in its self-consistent kinetic calculation of the electric structure of the injected particle front, thus offering an explanation for the fine spatial structure of the PJ/SAID phenomenon. This microscopic description of the front can supplement, in principle, any global magnetospheric electric field model that defines the overall convection pattern in which the injected plasma front is embedded. In particular, it could be incorporated into mod-

els based on the energy-dependent guiding center motion, which lead to the formation of a broadened Alfvén layer and the associated shielding currents [*Southwood and Wolf*, 1978; *Harel et al.*, 1981a, b; *Spiro et al.*, 1981].

The proposed scenario has profound implications for the dynamics of the ring current and the plasmasphere. A better understanding of the evolution of the injected particle front could clarify the origin of storm-time ring current enhancements [*Smith and Hoffman*, 1974; *Ejiri et al.*, 1980]. The scenario might contribute to an explanation of the observed penetration of the corotation electric field into the outer regions of the plasmasphere: Some plasma in the outer shells of the plasmasphere could be the remainder of plasma sheet material that has not yet acquired full corotation. The scenario also suggests that the PJ/SAID phenomenon plays a role in creating fine structure at the plasmapause, an idea that has been advanced before [*Spiro et al.*, 1981; *Ober et al.*, 1997].

Acknowledgments. The author thanks M. Roth, J. Lemaire, D. L. Carpenter, and Y. I. Galperin for many stimulating discussions, as well as E. Rigo for bibliographical assistance. The work described in this paper was performed at the Belgian Institute for Space Aeronomy and supported by the Belgian Office for Scientific, Technical and Cultural Affairs.

Michel Blanc thanks Yuri Galperin for his assistance in evaluating this paper.

References

Anderson, P. C., R. A. Heelis, and W. B. Hanson, The ionospheric signatures of rapid subauroral ion drifts, *J. Geophys. Res., 96*, 5785–5792, 1991.

Anderson, P. C., W. B. Hanson, R. A. Heelis, J. D. Craven, D. N. Baker, and L. A. Frank, A proposed production model of rapid subauroral ion drift and their relationship to substorm evolution, *J. Geophys. Res., 98*, 6069-6078, 1993.

Angelopoulos, V., W. Baumjohann, C. F. Kennel, F. V. Coronati, M. G. Kivelson, R. Pellat, R. J. Walker, H. Lühr, and G. Paschmann, Bursty bulk flows in the inner central plasma sheet, *J. Geophys. Res., 97*, 4027–4039, 1992.

Banks, P. M., and F. Yasuhara, Electric fields and conductivity in the nighttime E-region: A new magnetosphere-ionosphere-atmosphere coupling effect, *Geophys. Res. Lett., 5*, 1047–1050, 1978.

Block, L., On the distribution of electric fields in the magnetosphere, *J. Geophys. Res., 71*, 855–864, 1966.

Burch, J. L., S. A. Fields, and R. A. Heelis, Substorm effects observed in the auroral plasma, in *Physics of Solar Planetary Environments*, edited by D. J. Williams, vol. 2, pp. 740–759, AGU, Washington, D.C., 1976.

Carpenter, D. L., Whistler evidence of a 'knee' in the magnetospheric ionization density profile, *J. Geophys. Res., 68*, 1675–1682, 1963.

Comfort, R. H., Thermal structure of the plasmasphere, *Adv. Space Res., 17*(10), 175–184, 1996.

De Keyser, J., and M. Roth, Equilibrium conditions for the tangential discontinuity magnetopause, *J. Geophys. Res., 102*, 9513–9530, 1997.

De Keyser, J., M. Roth, and J. Lemaire, The magnetospheric driver of subauroral ion drifts, *Geophys. Res. Lett., 25*, 1625–1628, 1998.

Deminov, M. G., and V. N. Shubin, Dynamics of the subauroral ionosphere in disturbed conditions, *Geomagn. Aeron., 27*, 347–350, 1987.

Deminov, M. G., and V. N. Shubin, Electric field effects in the nighttime subauroral F region, *Geomagn. Aeron., 28*, 348–353, 1988.

Ejiri, M., R. A. Hoffman, and P. H. Smith, Energetic particle penetrations into the inner magnetosphere, *J. Geophys. Res., 85*, 653–663, 1980.

Filippov, V. M., D. D. Reshetnikov, V. L. Khalipov, V. S. Solovev, A. E. Stepanov, Y. I. Galperin, and T. M. Mulyarchuk, Coordinated measurements of narrow troughs of ionization in the F-region: Groundbased and satellite methods, *Kosm. Issled., 27*, 568–584, 1989.

Foster, J. C., M. J. Buonsanto, M. Mendillo, D. Nottingham, F. J. Rich, and W. Denig, Coordinated stable auroral red arc observations: Relationship to plasma convection, *J. Geophys. Res., 99*, 11,429–11,439, 1994.

Frank, L. A., W. R. Paterson, K. L. Ackerson, S. Kokubun, T. Yamamoto, D. H. Fairfield, and R. P. Lepping, Observations of plasmas associated with the magnetic signature of a plasmoid in the distant magnetotail, *Geophys. Res. Lett., 21*, 2967–2970, 1994.

Galperin, Y. I., V. N. Ponomarev, and A. G. Zosimova, Direct measurements of ion drift velocity in the upper atmosphere during a magnetic storm, *Kosm. Issled., 11*, 273–282, 1973.

Galperin, Y. I., V. L. Khalipov, and V. M. Filippov, Signature of rapid subauroral ion drifts in the high-latitude ionosphere structure, *Ann. Geophys., 4*, 145–154, 1986.

Gurevich, A. V., A. L. Krylov, and E. E. Tsedilina, Electric fields in the Earth's magnetosphere and ionosphere, *Space Sci. Rev., 19*, 59–160, 1976.

Harel, M., R. A. Wolf, P. H. Reiff, R. W. Spiro, W. J. Burke, F. J. Rich, and M. Smiddy, Quantitative simulation of a magnetospheric substorm, 1, Model logic and overview, *J. Geophys. Res., 86*, 2217–2241, 1981a.

Harel, M., R. A. Wolf, R. W. Spiro, P. H. Reiff, C.-K. Chen, W. J. Burke, F. J. Rich, and M. Smiddy, Quantitative simulation of a magnetospheric substorm, 2, Comparison with observations, *J. Geophys. Res., 86*, 2242–2260, 1981b.

Ho, C. M., B. T. Tsurutani, E. J. Smith, and W. C. Feldman, A detailed examination of a X-line region in the distant tail: ISEE-3 observations of jet flow and B_z reversals and a pair of slow shocks, *Geophys. Res. Lett., 21*, 3031–3034, 1994.

Jaggi, R. K., and R. A. Wolf, Self-consistent calculation of the motion of a sheet of ions in the magnetosphere, *J. Geophys. Res., 78*, 2852–2866, 1973.

Karlson, E. T., Plasma flow in the magnetosphere, *Cosmic Electr., 1*, 474–495, 1971.

Karlsson, T., G. T. Marklund, L. G. Blomberg, and A. Mälkki, Subauroral electric fields observed by the Freja satellite: A statistical study, *J. Geophys. Res., 103*, 4327–4341, 1998.

Kuznetsova, M. M., M. Roth, Z. Wang, and M. Ashour-Abdalla, Effect of the relative flow velocity on the structure and stability of the magnetopause current layer, *J. Geophys. Res., 99*, 4095–4104, 1994.

Lemaire, J., M. Roth, and J. De Keyser, High altitude electrostatic fields driving subauroral ion drifts, in *Magnetospheric Research With Advanced Techniques*, edited by R. L. Xu and A. T. Y. Lui, pp. 61–64, Elsevier Sci., New York, 1998.

Maynard, N. C., On large poleward-directed elecric fields at subauroral latitudes, *Geophys. Res. Lett., 5*, 617–618, 1978.

Maynard, N. C., T. L. Aggson, and J. P. Heppner, Magnetospheric observation of large sub-auroral electric fields, *Geophys. Res. Lett., 7*, 881–884, 1980.

McIlwain, C. E., Substorm injection boundaries, in *Magnetospheric Physics*, edited by B. M. McCormack, pp. 143–154, D. Reidel, Norwell, Mass., 1974.

McIlwain, C. E., A K_p dependent equatorial electric field model, *Adv. Space Res., 6*(3), 187–197, 1986.

Ober, D. M., J. L. Horwitz, and D. L. Gallagher, Formation of den-

sity troughs embedded in the outer plasmasphere by subauroral ion drift events, *J. Geophys. Res., 102*, 14,595–14,602, 1997.

Rich, F. J., W. J. Burke, M. C. Kelley, and M. Smiddy, Observations of field-aligned currents in association with strong convection electric fields at subauroral latitudes, *J. Geophys. Res., 85*, 2335–2340, 1980.

Rodger, A. S., R. J. Moffett, and S. Quegan, The role of ion drift in the formation of ionisation troughs in the mid- and high-latitude ionosphere: A review, *J. Atmos. Terr. Phys., 54*, 1–30, 1992.

Roth, M., J. De Keyser, and M. M. Kuznetsova, Vlasov theory of the equilibrium structure of tangential discontinuities in space plasmas, *Space Sci. Rev., 76*, 251–317, 1996.

Schunk, R. W., W. J. Raitt, and P. M. Banks, Effect of electric fields on the daytime high latitude *E* and *F* regions, *J. Geophys. Res., 80*, 3121–3130, 1975.

Shiokawa, K., C.-I. Meng, G. D. Reeves, F. J. Rich, and K. Yumoto, A multievent study of broadband electrons observed by the DMSP satellites and their relation to red aurora observed at midlatitude stations, *J. Geophys. Res., 102*, 14,237–14,253, 1997.

Smiddy, M., M. C. Kelley, W. Burke, F. Rich, R. Sagalyn, B. Shuman, R. Hays, and S. Lai, Intense poleward directed electric fields near the ionospheric projection of the plasmapause, *Geophys. Res. Lett., 4*, 543–546, 1977.

Smith, P. H., and R. A. Hoffman, Direct observations in the dusk hours of the characteristics of the storm time ring current particles during the beginning of magnetic storms, *J. Geophys. Res., 79*, 966–971, 1974.

Southwood, D. J., and R. A. Wolf, An assessment of the role of precipitation in magnetospheric convection, *J. Geophys. Res., 83*, 5227–5232, 1978.

Spiro, R. W., R. H. Heelis, and W. B. Hanson, Rapid subauroral ion drifts observed by Atmospheric Explorer C, *Geophys. Res. Lett., 6*, 657–660, 1979.

Spiro, R. W., M. Harel, R. A. Wolf, and P. H. Reiff, Quantitative simulation of a magnetospheric substorm, 3, Plasmaspheric electric fields and evolution of the plasmapause, *J. Geophys. Res., 86*, 2261–2272, 1981.

Whipple, E. C., J. R. Hill, and J. D. Nichols, Magnetopause structure and the question of accessibility, *J. Geophys. Res., 89*, 1508–1516, 1984.

Willis, D. M., The electrostatic field at the magnetopause, *Planet. Space Sci., 18*, 749–769, 1970.

Yeh, H.-C., J. C. Foster, F. J. Rich, and W. Swider, Storm time electric field penetration observed at mid-latitude, *J. Geophys. Res., 96*, 5707–5721, 1991.

J. De Keyser, Belgian Institute for Space Aeronomy, Ringlaan 3, B-1180 Brussels, Belgium. (Johan.DeKeyser@oma.be)

(Received April 15, 1998; revised February 1, 1999; accepted February 8, 1999.)